



Contents lists available at ScienceDirect

Forest Ecology and Management

journal homepage: www.elsevier.com/locate/foreco

Forest disturbance across the conterminous United States from 1985–2012: The emerging dominance of forest decline



Warren B. Cohen^{a,*}, Zhiqiang Yang^b, Stephen V. Stehman^c, Todd A. Schroeder^{d,1}, David M. Bell^a, Jeffrey G. Masek^e, Chengquan Huang^f, Garrett W. Meigs^g

^a Pacific Northwest Research Station, USDA Forest Service, Corvallis, OR 97331, USA

^b Department of Forest Ecosystems and Society, Oregon State University, Corvallis, OR 97331, USA

^c Department of Forest and Natural Resources Management, State University of New York, Syracuse, NY 13210, USA

^d Rocky Mountain Research Station, USDA Forest Service, Ogden, UT 84401, USA

^e Biospheric Sciences Laboratory, NASA Goddard Space Flight Center, Greenbelt, MD 20771, USA

^f Department of Geographical Sciences, University of Maryland, College Park, MD 20742, USA

^g Rubenstein School of Environment and Natural Resources, University of Vermont, Burlington, VT 05405, USA

ARTICLE INFO

Article history:

Received 25 August 2015

Received in revised form 21 October 2015

Accepted 25 October 2015

Available online 30 October 2015

Keywords:

Landsat time series

Forest disturbance estimation

Forest decline

TimeSync

Remote sensing

Probability sampling

ABSTRACT

Evidence of shifting dominance among major forest disturbance agent classes regionally to globally has been emerging in the literature. For example, climate-related stress and secondary stressors on forests (e.g., insect and disease, fire) have dramatically increased since the turn of the century globally, while harvest rates in the western US and elsewhere have declined. For shifts to be quantified, accurate historical forest disturbance estimates are required as a baseline for examining current trends. We report annual disturbance rates (with uncertainties) in the aggregate and by major change causal agent class for the conterminous US and five geographic subregions between 1985 and 2012. Results are based on human interpretations of Landsat time series from a probability sample of 7200 plots (30 m) distributed throughout the study area. Forest disturbance information was recorded with a Landsat time series visualization and data collection tool that incorporates ancillary high-resolution data. National rates of disturbance varied between 1.5% and 4.5% of forest area per year, with trends being strongly affected by shifting dominance among specific disturbance agent influences at the regional scale. Throughout the time series, national harvest disturbance rates varied between one and two percent, and were largely a function of harvest in the more heavily forested regions of the US (Mountain West, Northeast, and Southeast). During the first part of the time series, national disturbance rates largely reflected trends in harvest disturbance. Beginning in the mid-90s, forest decline-related disturbances associated with diminishing forest health (e.g., physiological stress leading to tree canopy cover loss, increases in tree mortality above background levels), especially in the Mountain West and Lowland West regions of the US, increased dramatically. Consequently, national disturbance rates greatly increased by 2000, and remained high for much of the decade. Decline-related disturbance rates reached as high as 8% per year in the western regions during the early-2000s. Although low compared to harvest and decline, fire disturbance rates also increased in the early- to mid-2000s. We segmented annual decline-related disturbance rates to distinguish between newly impacted areas and areas undergoing gradual but consistent decline over multiple years. We also translated Landsat reflectance change into tree canopy cover change information for greater relevance to ecosystem modelers and forest managers, who can derive better understanding of forest-climate interactions and better adapt management strategies to changing climate regimes. Similar studies could be carried out for other countries where there are sufficient Landsat data and historic temporal snapshots of high-resolution imagery.

Published by Elsevier B.V.

* Corresponding author.

E-mail addresses: wcohen@fs.fed.us (W.B. Cohen), zhiqiang.yang@oregonstate.edu (Z. Yang), svstehma@syr.edu (S.V. Stehman), tschroeder@usgs.gov (T.A. Schroeder), dmbell@fs.fed.us (D.M. Bell), jeffery.g.masek@nasa.gov (J.G. Masek), cqhuang@umd.edu (C. Huang), gmeigs@gmail.com (G.W. Meigs).

¹ Current address: ASRC Federal InuTeq, U.S. Geological Survey, Earth Resources Observation and Science Center, Sioux Falls, SD 57198, USA.

1. Introduction

Disturbance is a major driver of forest ecosystem dynamics, with the legacy of disturbance history being largely responsible for the state of a forest stand at any point in time (Uuttera et al., 1996; Pflugmacher et al., 2012). Disturbances can alter the mix of species and stand structure in ways that depend on disturbance agent (e.g., fire, harvest, insects) and severity or magnitude, with variable and profound implications on fluxes of water, energy, and nutrients, biodiversity, and a host of other functions that strongly influence life on earth (Edwards et al., 2014). There is evidence that in the past several decades patterns of forest disturbance among disturbance causal agent classes have begun to shift both regionally and globally. For example, in the western US, timber harvesting on public lands has decreased (Oswalt et al., 2014) while forest fire frequencies have increased (Westerling et al., 2006). Across Europe, wildfire, wind, and bark beetle disturbances have steadily increased since the early 1970s (Seidl et al., 2014). Globally, incidents of both chronic and acute forest decline, purportedly related to climate change, have become increasingly common (Allen et al., 2010). Because of the importance of disturbance on forest function and implications for shifting dominance among classes of disturbance agent, ecological modeling and natural resource decision-making can benefit from improved national- to continental-scale monitoring and assessments (Running, 2008).

Currently, much of what we know about forest disturbance comes from disparate monitoring efforts that produce estimates that are challenging to compare and synthesize across disturbance agent classes, regions, and time periods. Further, estimates of disturbance rates produced by these efforts are often biased. For example, in the case of remote sensing based approaches if image spatial resolution is too coarse to capture small-scale disturbance these omission errors of disturbance will lead to bias in the area estimates. In general, map classification error, which is always present to some extent, also leads to biased area estimates (Olofsson et al., 2013). In the US several monitoring programs focus on forest disturbance but as a collection these are lacking in sufficient detail and temporal record length. US forest inventory data are able to resolve all major disturbance agent classes (Schroeder et al., 2014), but these data have only been collected in a nationally consistent manner for a little over a decade and have long re-measurement periods (i.e., 5 years in the east and 10 years in the west). The ForWarn system (Norman et al., 2013) is designed to detect and map an array of disturbance agent classes at a sub-monthly time step. ForWarn relies on MODIS data which has a spatial resolution (250 m) that is incapable of resolving many stand-scale events. Further, ForWarn extends temporally back only to 2000. Although the LANDFIRE program derives disturbance maps across disturbance agent classes at a 30 m nominal resolution, LANDFIRE also extends back only to 1999 (Vogelmann et al., 2011). Several other major monitoring programs report only a limited set of disturbance agent classes and often have significant measurement bias. For example, aerial insect and disease detection surveys (ADS) use visually defined polygons that only approximate area affected and are not collected everywhere every year (Meddens et al., 2012). The US fire mapping program, Monitoring Trends in Burn Severity (MTBS; Eidenshink et al., 2007), is based on Landsat data but maps only larger fire size events (~200 ha in the east, ~400 ha in the west).

The Landsat satellite remote sensing program holds great promise to satisfy monitoring needs because it provides one of the few datasets capable of quantifying diverse patterns and dynamics of forests at sub-stand scales and at sub-annual temporal resolution over the last several decades (Banskota et al., 2014).

The spatial resolution of most Landsat data is 30 m, and with two satellites active over much of the life of the Landsat program (1972–present), data have been collected globally at either an 8- or 16-day interval, providing at least one clear view of the earth's surface during the growing season every year in most places (Roy et al., 2014). Data are free of charge and available from the archive in calibrated, georeferenced, and analysis-ready format (Woodcock et al., 2008). There are well-established protocols using Landsat data to map forest disturbance across all forest types globally (Cohen and Goward, 2004; Hansen et al., 2013) using data from the full temporal depth of the archive (Cohen et al., 2002). Moreover, there has been recent rapid development of sophisticated algorithms designed to use all available imagery in time series change detection analyses, offering great opportunities for the future of Landsat-based science (Huang et al., 2010; Kennedy et al., 2010; Brooks et al., 2014; Zhu and Woodcock, 2014). Additionally, we are now making good progress toward full integration of early Landsat data (MSS starting in 1972) in time series analyses (Braaten et al., 2015). This is important because the MSS data, despite presenting distinct challenges in time series analysis, would extend the record of forest dynamics backwards an additional 12 years.

Unfortunately, the full promise of automated Landsat disturbance mapping has yet to be realized. For example, Hansen et al. (2013) and Masek et al. (2013) provided national, annual data but quantified mostly moderate to high-severity, short-duration disturbances only and did not distinguish among disturbance agent classes. Meddens and Hicke (2014) and Meigs et al. (2015) targeted more gradual phenomena associated with insect disturbances, but these studies were limited in geographic scope. Zhu and Woodcock (2014) and Kennedy et al. (2015) evaluated a more comprehensive set of disturbance agent classes, but results were likewise spatially limited.

Recently, McDowell et al. (2015) described a comprehensive monitoring framework required for systematic quantification and analysis of disturbance that transcends limitations of current monitoring systems. The first two of the four primary framework components, detection and disturbance agent classification, emphasize a strong role for remote sensing. In this context, detection ranges from partial canopy loss to tree mortality and should be based on sub-patch scale observations at an annual or less time-step. Disturbance classification includes such agents as harvest, fire, insects, etc. Implied is that consistent (or at least harmonious) methods that allow comparison and integration of estimates should be used to detect disturbances across agent classes through time and over space. To improve the use of remote sensing for forest disturbance monitoring, we further suggest that the estimates of area and rates of disturbance be unbiased, include uncertainties, and have a long enough retrospective monitoring period to allow current trends to be contrasted against the recent past. Only then can we detect and quantify meaningful shifts in dominance among major causal agent classes.

The objective of our study is to characterize forest disturbance by major causal disturbance agent class for the conterminous US during the time period 1985–2012. We implement a disturbance monitoring strategy that is temporally and spatially consistent to allow comparisons of disturbance rates and agent classes across regions and time periods. In addition, we assess how the dominance among various disturbance agent classes has shifted, both nationally and regionally, between 1985 and 2012 across the full range of disturbance severities (or magnitudes). Rates of disturbance along with causal agent classes are quantified by visual interpretation of Landsat time series, and regional and national disturbance rates (by time period) are estimated from a probability sample of 7200 pixel-level observations distributed across the

conterminous US. The adequacy of the sample size for the regional and national estimates can be assessed by examining the standard errors associated with each estimate.

2. Materials and methods

2.1. Sample design

For efficiency in preparing imagery for interpretation, we used Landsat scenes of the second World Reference System (WRS2) as clusters in a two-stage stratified cluster design. Scenes (Fig. 1) were defined as the non-overlapping portions of individual frames known as TSAs (Thiessen Scene Areas; Kennedy et al., 2010). Of the 442 individual TSAs covering the conterminous US, we selected 180 for the sample, a data volume deemed manageable at the start of this study. Stratified sampling was implemented because we wanted a higher proportion of the sampled TSAs to be drawn from forested regions. Strata were based on a combination of the EPA Level II ecoregion map (Omernik, 1987) and the US Forest Service forest type map (Ruefenacht et al., 2008). Using these two maps, the ecoregions were generalized into five coarser strata that combined different ecoregions sharing similar forest types (Table 1). Five regional strata were defined – Mountain West, Lowland West, Central, Northeast, and Southeast – and the dominant regional stratum was assigned as the label for each TSA (Fig. 1). To determine the allocation of the 180 TSAs to strata, we calculated the product of forest area per regional stratum (from the forest type map within TSA boundaries) and stratum area, as represented by the sum of area across the collection of TSAs in that stratum. Summing the regional product values and determining the proportional contribution of each product value to the summation of values yielded the proportion of the 180 TSA clusters sampled per stratum. From the 58, 86, 127, 84, and 87 TSAs from the Mountain West, Lowland West, Central, Northeast, and Southeast strata, respectively, we selected 42, 18, 14, 52, and 54 via simple random sampling within each stratum (Fig. 1). For example, even though the Central stratum has the largest areal proportion across the US (~30%), because it had a small forest area (8.2%), fewer sample clusters were selected for that stratum than for other, more forested strata.

For the second stage of the sample design, within each of the 180 first-stage sample TSAs, we selected a simple random sample of 40 Landsat plots (30 m pixels) to be interpreted, resulting in a sample size of 7200 (the number of sample locations we could afford to interpret). We refer here to our sample units as Landsat plots, following the long-used practice of assessing photo plots for inventory and related purposes when aerial photos are used to collect data as part of a sample design in forestry. No further stratification (e.g., forest and nonforest) was used in the second-stage sample selection protocol.

2.2. Landsat plot data collection

Each of the 7200 Landsat plots was first interpreted to determine if it was forested at any time during the period of observation. Similar to the US forest inventory, here forest was defined as planted or naturally vegetated land likely to contain 10% or greater tree cover that was not an agricultural crop (e.g., orchard) at some time during a near-term successional sequence. Because of land use conversions, some plots were forested only a portion of the time period of this study. Forest management (e.g., harvest) and natural disturbances (e.g., fire, insects) that did not result in a land use change were labeled as forest throughout the time period of observation. We noted conversions of land use (forest to non-forest and the reverse), as well as the timing of those conversions, so that we could accurately derive annual area of forest for annual disturbance rates estimates (Section 2.3).

Forest disturbance occurrence was interpreted using the Landsat time series visualization and disturbance data collection software (TimeSync) that integrates several important features to assure high quality data collection (Cohen et al., 2010): simultaneous viewing of Landsat time series around a Landsat plot of interest, rapid toggling to view multiple spectral band and index time series graphical plots (i.e., temporal trajectories), and temporal snapshots of high resolution imagery in Google Earth. Using a nearly identical set of tools to collect disturbance data and comparing results against forest inventory data, Schroeder et al. (2014) substantiated the validity of the TimeSync approach for collecting highly accurate disturbance information via visual interpretation of Landsat time series.

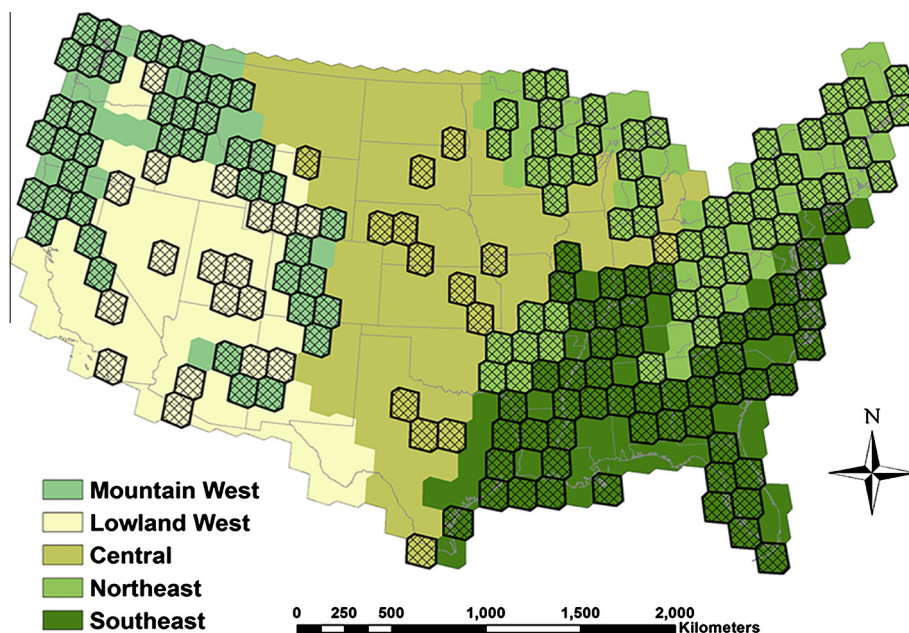


Fig. 1. Regionalized stratification of Landsat Thiessen Scene Areas (TSAs) for the conterminous US derived from a combination of ecoregion and forest type maps (as described in text). TSAs selected in the sample are shown with thicker border lines and crosshatching.

Table 1
Level II ecoregions and forest type groups contained within each regional stratum.

Stratum (percent forested)	Level II ecoregion ^a	Forest type group (percent of total) ^b
Mountain West (62.5)	Marine West Coast Forest, Western Cordillera, Northwestern Forested Mountains, Western Sierra Madre	Douglas-fir (26.9), Fir/Spruce/Mountain Hemlock (19.6), Ponderosa Pine (14.3), Pinyon/Juniper (10.9), Lodgepole Pine (8.8), California Mixed Conifer (5.6), Aspen/Birch (3.8), Western Oak (3.4), Hemlock/Sitka Spruce (2.3), Other Western Softwoods (1.3), Alder/Maple (1.0), Tanoak/Laurel (1.0)
Lowland West (16.8)	Cold Deserts, Warm Deserts, Mediterranean California, Upper Gila Mountains	Pinyon/Juniper (72.7), Western White Pine (12.8), Ponderosa Pine (4.1), Exotic Hardwood (3.0), Western Oak (2.0), Redwood (1.5), Tanoak/Laurel (1.5)
Central (8.2)	South Central Semiarid Prairies, Western Central Semiarid Prairies, Temperate Prairies, Central USA Plains, Tamaulipas-Texas Semiarid Plains	Oak/Hickory (54.0), Elm/Ash/Cottonwood (9.8), Loblolly/Shortleaf Pine (7.5), Ponderosa Pine (6.6), Pinyon/Juniper (6.2), Oak/Pine (6.0), Maple/Beech/Birch (3.4), Aspen/Birch (3.2), Oak/Gum/Cypress (1.8)
Northeast (61.4)	Ozark-Ouachita Appalachian Forest, Mixedwood Plains, Mixedwood Shields, Atlantic Highlands	Oak/Hickory (45.4), Maple/Beech/Birch (24.5), Aspen/Birch (12.1), Spruce/Fir (8.4), White/Red/Jack Pine (3.7), Loblolly/Shortleaf Pine (3.0), Oak/Pine (1.4), Elm/Ash/Cottonwood (1.0)
Southeast (53.7)	Southeastern USA Plains, Mississippi Alluvial and Southeast USA Coastal Plains, Texas-Louisiana Coastal Plains, Everglades	Loblolly/Shortleaf Pine (35.1), Oak/Hickory (30.4), Oak/Gum/Cypress (14.0), Longleaf/Slash Pine (9.8), Oak/Pine (7.9), Elm/Ash/Cottonwood (2.3)

^a Type groups (from Rufenacht et al., 2008) having less than 1% of total omitted.

^b From Omernik, 1987.

Interpretations were made at an annual time step for each of the Landsat plots (following Cohen et al., 2010; Pflugmacher et al., 2012) labeled as forest use at any time during the period of observation (3861). Several metrics of disturbance were derived from the primary interpretations. Year of disturbance detection (YOD) was the first year a given disturbance was detected. For example, for a disturbance lasting one year and occurring between 1984 (first year of Landsat imagery used) and 1985, YOD was 1985. Magnitude of disturbance was calculated as the relative amount of reflectance change associated with the disturbance. Relative reflectance change magnitude was expressed in terms of the Tasseled Cap angle index, as the difference between the start and end angle values, divided by the start vertex angle value. This index, first described by Powell et al. (2010) and used by Gómez et al. (2011) and Pflugmacher et al. (2012) for time series analyses, is related to the more common Normalized Difference Vegetation Index (NDVI) but has greater sensitivity at higher percent vegetation cover proportions. Duration of change was recorded for all disturbance occurrences, and had a value from one to n , where n is the number of consecutive years that a given disturbance occurrence or process lasted in the given Landsat plot. Most disturbance occurrences lasted one year (e.g., fire, harvest, wind), but sometimes harvest and usually forest decline were multi-year processes. A multi-year disturbance for a given Landsat plot implicitly means that separate portions of the plot were disturbed over a period of years, and includes progressive losses of leaf area or canopy cover within specific, affected trees over several growing seasons.

Table 2
Descriptions of disturbance causal agent classes interpreted with TimeSync on forested plots.

Causal agent class	Description
Harvest	Apparent removal of tree stems by mechanical means, where land use was forest before and after removal
Fire	Evidence of burning from either natural (wildfire) or anthropogenic (prescribed burning) causes
Decline	Either temporary (one year or less) or longer-term (two or more years duration) tree canopy cover loss not associated with the harvest, fire, or other classes. The specific agent could not easily be determined, but likely included insects, diseases, and physiological stresses that reduced canopy cover or leaf area density, or killed whole trees within a Landsat plot
Other	Includes several subclasses: <ul style="list-style-type: none"> • Wind – Evidence of wind damage from hurricanes, tornadoes, and storms • Water – Tree mortality associated with flooding • Land use change – When forest was converted to non-forest • Debris – When tree canopy cover was destroyed by natural material movement associated landslides and avalanches

For each disturbance occurrence or process, apparent causal agent class (Table 2) was interpreted in TimeSync with the aid of high spatial resolution imagery available in Google Earth, as well as ancillary databases of fire, wind, insect and disease, and management activity data available from various government agencies (Table 3). The harvest class involved mechanical removal of trees, and fire included both wildfire and prescribed burning. The causal disturbance agent class “other” was dominated by land use conversion but included disturbances from wind, water, debris, and unknown causes. The specific causal agent driving the decline class could not be determined from our observations, but is generally known to be associated with insects, disease, and physiologically induced stress caused by excessive temperatures often combined with short-term or extended drought where not all trees present are equally affected at the same time (Amoroso et al., 2012; Choat et al., 2012; Meddens and Hicke, 2014; Vilà-Cabrera et al., 2013; Anderegg et al., 2015; Meigs et al., 2015). We labeled as decline any observation where we determined there was a general loss of canopy leaf area density not associated with management, fire, or other defined agents (Table 2). Rapid decline, when noted, was commonly associated with eastern deciduous broadleaf forests that were under apparent broad scale attack by leaf eating insects (commonly followed by rapid recovery in subsequent years). This was determined from the convergence of visual evidence available in TimeSync, backed up by referencing temporal and spatial patterns of insect and disease observations available from ADS data. Gradual decline was far more common, especially in western conifer forests, and usually, but not always, resulted in mortality of some trees within a plot and was associated with ADS insect and disease observations. Gradual decline was assessed by examining both the annual reflectance trends (trajectories) in multiple spectral bands and indices and Landsat image coloration changes associated with those trends in the plot and its immediate neighborhood. A subsequent high-resolution image snapshot available in Google Earth was used for confirmation.

2.3. Estimation of annual disturbance area and rate

The estimates of areas and rates of disturbance from the sample of plots for a given year were produced using the SURVEYMEANS procedure of the Statistical Analysis Software (SAS version 9.3, SAS Institute Inc., Cary, North Carolina, USA). For the sampling

Table 3
Ancillary databases used to identify or confirm causal agent class associated with observed disturbances.

Database webpage	Description
foresthealth.fs.usda.gov/portal/Flex/IDS	US Forest Service aerial detection survey map database containing information about approximate locations and timing for a variety of specific insects and diseases for conterminous US (predominantly since 1997)
www.nws.noaa.gov/gis/shapepage.htm	US National Weather Service database giving approximate locations of specific high intensity weather events
www.mtbs.gov	Landsat-based database for all significant fires across all lands in the US from 1984 to 2014
www.fs.fed.us/nrm/index.shtml	Information on access to US Forest Service database for all treatment activities

design implemented, the primary sampling unit is a TSA (indicated by the subscript i) and each TSA is associated with a stratum h . A ratio estimator is used to estimate the proportion of forest area that is disturbed, where the proportion is defined as area of disturbed forest divided by total area of forest,

$$\hat{R} = \frac{\sum_{h=1}^H \sum_{i=1}^{k_h} \sum_{j=1}^{n_{hi}} w_{hij} y_{hij}}{\sum_{h=1}^H \sum_{i=1}^{k_h} \sum_{j=1}^{n_{hi}} w_{hij} x_{hij}} \quad (1)$$

and h is the stratum index, i is the TSA index in stratum h for the sample size of k_h TSAs sampled from the K_h TSAs available in stratum h ($i = 1, 2, \dots, k_h$), j is the index of a sampled pixel ($j = 1, \dots, n_{hi}$), n_{hi} is the number of pixels sampled from the N_{hi} pixels available in cluster i of stratum h , and w_{hij} is the estimation weight (i.e., inverse of the inclusion probability) for sample pixel j in TSA i of stratum h . The variable x_{hij} is the area of forest in sample pixel j from TSA i of stratum h , and y_{hij} = area disturbed (e.g., a disturbed pixel would have disturbed area of 900 m² whereas $y_{hij} = 0$ if the pixel is not disturbed forest). Note that the 900 m² area is the finest resolution observed, but the full area of the pixel need not have been disturbed for that pixel to be identified as disturbed. The numerator of Eq. (1) based on y_{hij} is the estimated total area of disturbed forest.

For the two-stage cluster sampling design, the inclusion probability of a pixel is the product of the first-stage inclusion probability (k_h/K_h) and the second-stage inclusion probability ($40/N_{hi}$). The second-stage inclusion probability is a conditional probability in which the conditioning is on the sample of TSAs selected at the first stage, and this conditional probability is determined for a simple random sample of 40 pixels selected from the N_{hi} pixels available in sampled TSA i of stratum h .

The variance estimator for \hat{R} provided by SAS is based on a Taylor series approximation (Särndal et al., 1992) (see SAS version 9.3 documentation for Statistical Computations of the SURVEYMEANS procedure). The SAS algorithm for variance estimation for two-stage cluster sampling does not incorporate the within primary sampling unit variance component associated with the second-stage sample so the standard errors reported represent slight underestimates.

2.4. Conversion of spectral change to tree canopy cover change

Remote sensing-based forest disturbance estimates have historically been reported as rates or areas of disturbance over a given time period, without accompanying descriptions of disturbance severity or magnitude (Cohen et al., 2002; Hansen et al., 2013; Masek et al., 2008, 2013). When magnitude has been reported, it was commonly in terms of reflectance change (Skakun et al., 2003) or total vegetation cover change (Kennedy et al., 2012), including herbaceous and shrub components. Because we report

annual forest canopy disturbance at the 30 m pixel resolution and knowingly include partial pixel disturbances, sometimes accumulating over multiple consecutive years within a given Landsat plot, we wanted to also report magnitudes in terms of cumulative tree canopy cover loss. To accomplish this, we related spectral change to tree canopy cover change using 21,950 photo interpreted tree canopy cover plots from Coulston et al. (2012) and the Random Forests regression tree algorithm (Breiman, 2001) to predict tree canopy cover through time for all the disturbed Landsat plots described above in Section 2.2.

Tree canopy cover was predicted as a function of contemporaneous Tasseled Cap brightness, greenness, and wetness, and regional stratum (the five regions of Fig. 1) as predictors ($R^2 = 0.58$, and slope of observed versus predicted from leave-one-out cross validation = 1.06). This model was applied to the pre-disturbance and post-disturbance reflectance data (over the full duration if more than one year), and the predictions were differenced to calculate the tree canopy cover change for each disturbance observation over the duration. For multi-year disturbances, dividing by duration can yield annual cover change. Although differencing can amplify tree cover change prediction error, it is a long-standing approach for modeling change with reflectance data (Healey et al., 2006; Powell et al., 2014), yielding results nearly equivalent to modeling cover change directly from reflectance change. For our application, the tree canopy change predictions were meaningful if they could generally distinguish different levels of cover change among agent classes, even if the actual change values were somewhat inaccurate.

3. Results

3.1. National and regional aggregate disturbance rates

Estimated area of disturbed forest across the conterminous US averaged 8.4 ± 0.73 million ha per year between 1985 and 2012 (SE = 0.73 is the average of annual SE estimates). The percent of forest area disturbed each year was highly variable, with a remarkable increase beginning in the mid-90s (“all” in Fig. 2 for the US). For the first 10 years of the series (1985–1995), the rate of disturbance averaged $1.76 \pm 0.17\%$ per year. Between 1995 and 2001 the rate more than doubled, rising steadily during that period. In 2006 the disturbance rate peaked at $4.69 \pm 0.30\%$ and thereafter began a downward trend, ending the time series in 2012 at $3.44 \pm 0.33\%$.

Temporal variability in national disturbance rates was strongly related to regional disturbance patterns. In the Northeast region, rates increased steadily, albeit only slightly over time (0.05% per year), averaging $1.93 \pm 0.30\%$ over the full period of observation (all, Fig. 2, Northeast). Rates in the Southeast region were variable but with no clear trend throughout the period, averaging $3.38 \pm 0.38\%$ per year (all, Fig. 2, Southeast). In the Lowland West (all, Fig. 2, Lowland West) and Mountain West (all, Fig. 2, Mountain West) regions, disturbance rates increased dramatically after the early-90s. The Lowland West region had disturbance rates near zero until 1995, which then climbed steadily at a rate of 1.08% per year, peaking at $9.21 \pm 2.14\%$ in 2002. After 2002, disturbance rates in this region dropped as precipitously as they had increased until 2005, after which they varied between 2% and 4% per year. The disturbance rate pattern for the Mountain West was similar in part to that of the Lowland West region, where rates dramatically increased during the latter half of the 90s (1.07% per year). Between 2000 and 2008, rates of disturbance remained above 8.7%, peaking at $9.61 \pm 0.97\%$ in 2003. After 2008, rates declined at about the same rate as they increased, but appeared to level off at a rate above 6% by 2012. Disturbance rates for the Central region were quite low throughout the entire time series and are not reported here.

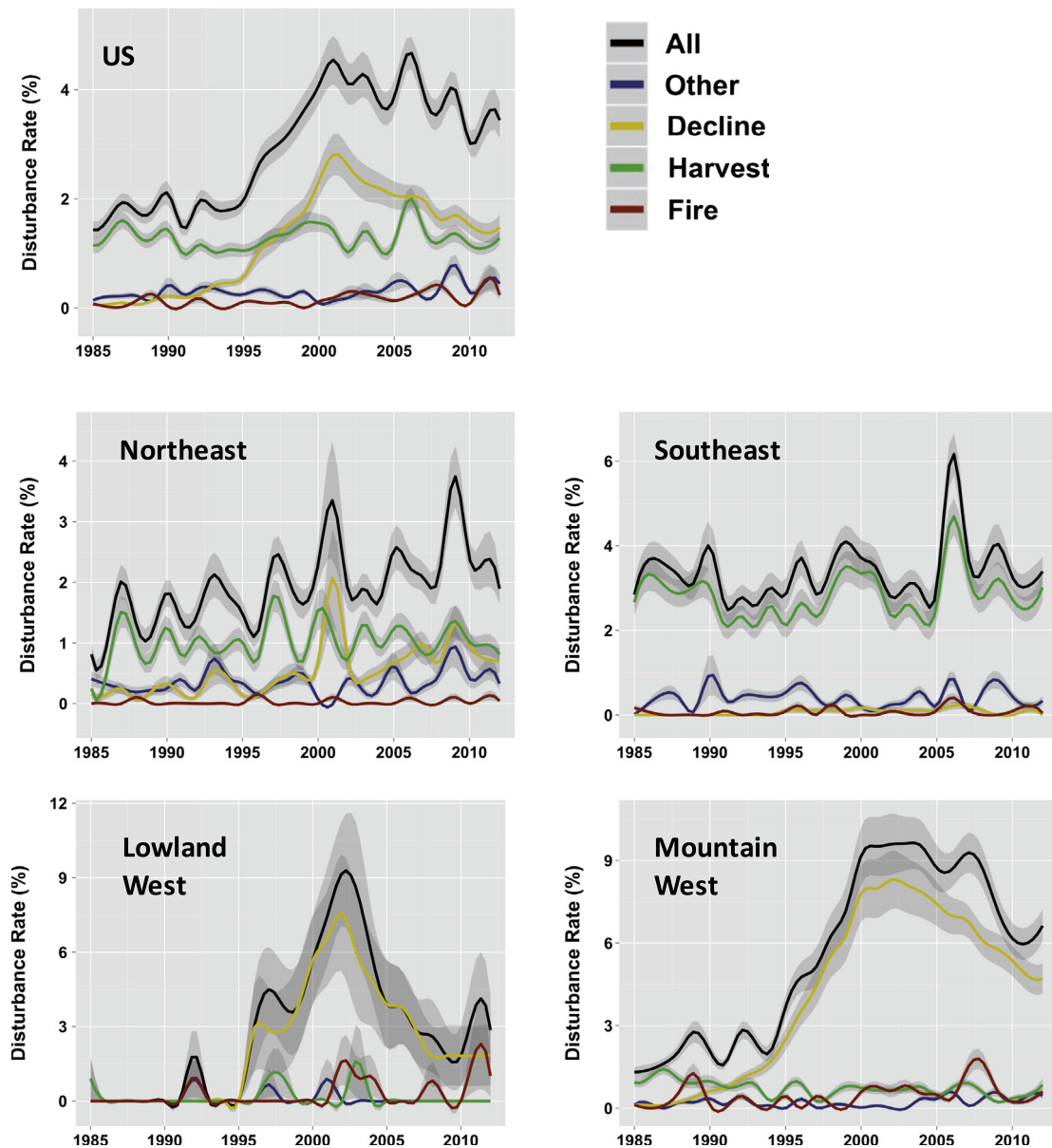


Fig. 2. Annual rates of forest disturbance (smoothed lines with 1 SE envelopes), for all disturbance classes (All) and by major causal agent class, across the conterminous US and by region.

3.2. National and regional disturbance rates by disturbance agent class

Disaggregating national total disturbance rates by causal agent class revealed that decline-related disturbances were largely responsible for the dominant temporal trend of the national rate (Fig. 2, US). The rate of disturbance for the decline class of agents steadily increased from 1985 ($0.07 \pm 0.02\%$) through 2001 ($2.82 \pm 0.38\%$). Two notable periods were 1985–1995, when the rate of increase was 0.05% per year, and 1995–2001 when the rate of increase was seven times higher (0.35% per year). After 2001, decline-related disturbance decreased at a rate of 0.12% per year through 2011 (roughly half the rate at which it increased post-1995), remaining relatively high at $1.48 \pm 0.23\%$ in 2012. In contrast, although harvest was somewhat variable over time ($1.28 \pm 0.14\%$), there was no sustained trend. Fire exhibited low rates of disturbance across time, but did display lower rates before 2000 ($0.08 \pm 0.03\%$) than after 2000 ($0.24 \pm 0.07\%$). The agent class

other had slightly higher rates than fire ($0.29 \pm 0.07\%$) with no meaningful increase over time.

Disturbance rates among causal agent classes were highly variable by region. In the eastern regions, harvest was the dominant agent throughout most of the full observation period. In the Southeast, although temporally variable (high of $4.67 \pm 0.43\%$ in 2006, low of $2.08 \pm 0.27\%$ in 1993), the mean harvest rate was $2.90 \pm 0.34\%$ per year, far above the rates for other agent classes (Fig. 2, Southeast). Harvest was lower and less variable in the Northeast ($1.01 \pm 0.19\%$ per year), but was still the dominant agent class for most of the observation period (Fig. 2, Northeast). The rate of harvest in the Mountain West decreased 0.06% per year from 1985 ($0.93 \pm 0.16\%$) to 1997 ($0.27 \pm 0.08\%$). Between 1997 and 2012 the harvest rate was somewhat erratic, averaging $0.61 \pm 0.14\%$ with a high of $0.92 \pm 0.14\%$ in 2007 and a low of $0.23 \pm 0.07\%$ in 2009. In Lowland West harvest rates were generally low throughout the study period, except in a few specific years.

In the western regions, forest decline was the most important causal disturbance agent class, especially after the early 90s. In the Lowland West (Fig. 2, Lowland West), decline-related disturbance was only rarely observed before 1996, after which it rapidly became the dominant class rising at an average rate of 0.96% per year until its peak in 2002 at $7.57 \pm 2.38\%$. Between 2002 and 2008, a decreasing rate of 0.87% per year was observed, before the rate of decline-related disturbance stabilized at an average rate of $1.83 \pm 1.22\%$ per year between 2008 and 2012. In the Mountain West (Fig. 2, Mountain West), forest decline was notably expressed in three distinct periods. Between 1985 and 1995, there was a slow but steady increasing rate (0.22% per year), which accelerated after 1995 (at an increasing rate of 1.03% per year) until 2000. From 2000 to 2003, that rate varied between $7.81 \pm 1.02\%$ and $8.30 \pm 1.06\%$, after which time forest decline decreased at a rate of 0.40% per year. By 2012 decline-related disturbance was still high, at $4.71 \pm 0.55\%$. Forest decline occurred at low rates in the Southeast ($0.07 \pm 0.06\%$ Fig. 2, Southeast). In the Northeast decline was a more important causal agent class ($0.53 \pm 0.17\%$, Fig. 2, Northeast), exhibited by a marked increase after about 1997 ($0.22 \pm 0.10\%$ and $0.79 \pm 0.22\%$, before and after 1997, respectively), and a large pulse resulting in a high of $2.08 \pm 0.81\%$ reached in 2001.

When viewed in the aggregate, fire, although regularly occurring, was a minor disturbance agent relative to harvest and forest decline. Fire was common in the Mountain West (Fig. 2, Mountain West) throughout the period of observation but varied episodically. After 2000 the rate became elevated through about 2008, peaking at $1.71 \pm 0.34\%$ in 2008. In the Lowland West (Fig. 2, Lowland West) the most prominent fire disturbance years occurred after 2001, with the period between 2002 and 2004 being the most active, peaking at $1.64 \pm 0.98\%$ in 2002. The three other most active fire years were 2008 ($0.82 \pm 0.77\%$), 2011 ($2.02 \pm 1.59\%$), and 2012 ($1.01 \pm 0.84\%$). In the Southeast (Fig. 2, Southeast) fire was a regular feature, albeit with no remarkable temporal patterns ($0.09 \pm 0.04\%$). Fire in the Northeast (Fig. 2, Northeast) was somewhat regularly occurring but only at low rates, averaging $0.03 \pm 0.02\%$ over the full period. The agent class other was minimal in the west, but more important than fire in the east. In the Southeast (Fig. 2, Southeast) no trend was evident for the other class with rates averaging $0.40 \pm 0.13\%$. In the Northeast (Fig. 2, Northeast) rates were similarly low ($0.34 \pm 0.12\%$) and without an obvious trend.

3.3. Disturbance rates by reflectance magnitude and tree canopy cover change

As noted above, magnitude of disturbance in reflectance space was quantified using the Tasseled Cap angle metric. Distributions of annual spectral change magnitudes were highly variable by agent, with the majority of disturbances having relative spectral changes less than 50% (Fig. 3, top). Fire had the highest change magnitudes, with a median of 38.1%. This was followed by the agent classes harvest and other, at 21.7% and 20.1%, respectively. Decline had the lowest change magnitudes, with a median of 1.5% per year.

Disturbance duration was one year for fire, mostly one year for harvest and other, but generally multi-year for forest decline (Table 4). There were dramatic differences for decline between the eastern and western regions (data not shown). In the eastern regions, 86% of all decline-related disturbances had durations of less than 5 years. In the western regions 68% of decline occurrences had durations lasting 5 or more years and 24% had durations 10 or more years in length.

For a more direct comparison of tree cover changes among the four agent classes, we report tree canopy cover change

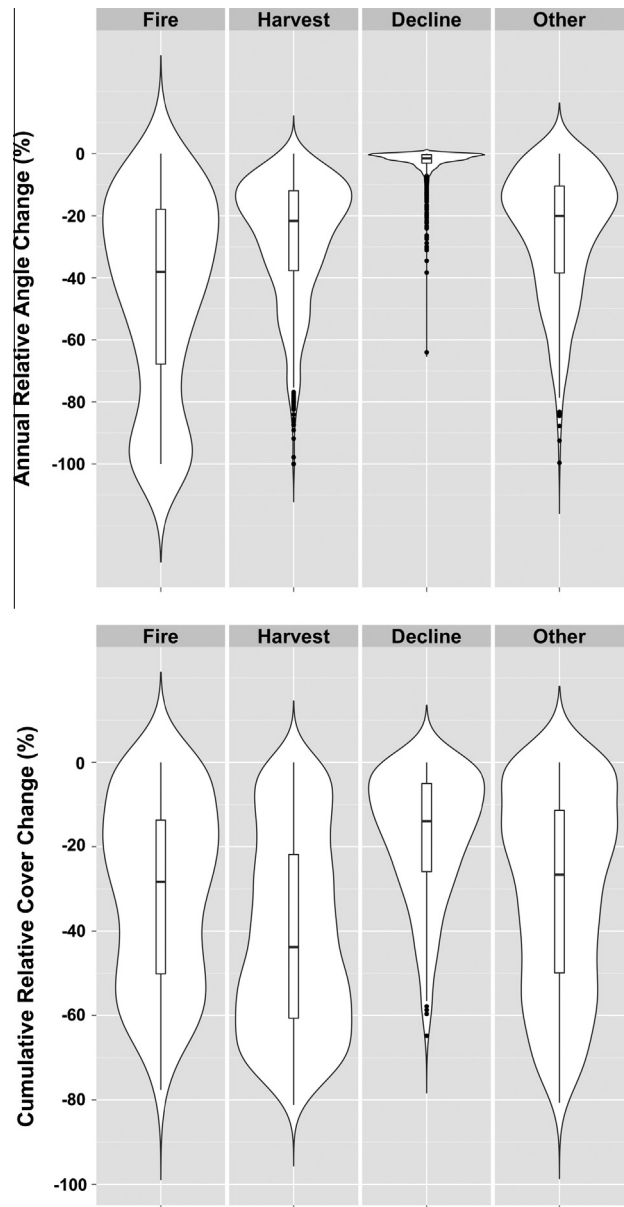


Fig. 3. Violin plots by disturbance causal agent class of annual relative angle change magnitude (top), and cumulative relative tree canopy cover change (bottom).

Table 4

Number of disturbance occurrences by disturbance agent class and duration for the forested Landsat plots used in this study. The Total column represents the number of affected plots in a given class, whereas the Percent column represents the proportions of total occurrences represented by a given class (or subclass for the class Other).

Agent	Duration (years)					Total	Percent
	1	2	3	4	5+		
Fire	167	0	0	0	0	167	7.60
Harvest	1319	88	4	2	0	1413	64.29
Decline	69	13	17	20	115	230	10.46
Other	340	36	9	3	0	388	17.65
Debris	1	0	0	0	0	1	0.05
Land use	216	28	4	0	0	248	11.28
Water	13	2	1	0	0	16	0.73
Wind	61	0	0	0	0	61	2.78
Unknown	49	6	4	3	0	62	2.82
Total	1891	137	30	25	115	2198	100.00
Percent	86.03	6.23	1.36	1.14	5.23	100.00	-

distributions as accumulated values over the observed duration for a given disturbance occurrence. Cumulative tree cover change distributions were highly variable within an agent class, but generally lower than 50%, especially for forest decline (Fig. 3, bottom). Harvest had the highest median cumulative relative cover change, followed in descending order by fire, other, and decline.

4. Discussion

4.1. Shifting dominance of disturbance agent classes over time

We report forest disturbance rates for the conterminous US across major causal agent classes at an annual time step between 1985 and 2012, emphasizing the shifting importance among disturbance agent classes during recent decades (Fig. 2). Prior to the mid-90s, national disturbance rates varied between 1.5% and 2% per year, driven largely by harvest activity, primarily in the Mountain West, Northeast, and Southeast regions. During the late-80s and early-90s, harvest rates decreased in the Mountain West, but decline-related disturbances increased rapidly in the two western regions. After 1997, the decline class dominated national disturbance rates, with the greatest disparity occurring during the early 2000s, when forest decline varied between 2% and nearly 3%. A slow but steady decreasing rate of forest decline after its peak in 2002 brought this agent class into near parity with harvest by 2012, at rates considerably higher than pre-1995 rates.

Oswalt et al. (2014; Table 3), reported a 9% decrease in the rates of tree mortality for the conterminous US over the 20 years between 1976 and 1996 followed by a 68% increase between 1996 and 2006, and then a slower increase (15%) through 2011. These inventory-based results report tree mortality as a percentage of growing stock, rather than the more comprehensive characterization of decline used here, but clearly corroborate our estimates of a major contrast in decline prior to the mid-90s with decline between the mid-90s and the mid-2000s, followed by subsequent slower rates of decline. Moreover, these data support our observations that the highest rates of increased decline-related disturbance occurred in our western regions: 180% increase in mortality between 1996 and 2006 in the Oswalt et al. (2014) Rocky Mountain and Pacific Coast regions. Similar to our decline results, as compared to the western US, in our Northeast region Oswalt et al. (2014) reported lower rates of mortality (4% per year) over the 15 years from 1996 to 2011. For our Southeast region, Oswalt et al. (2014) reported half the Northeast rate of increase, again consistent with our decline results.

Aerial Detection Survey data (Table 3) are based on methods that have some similarities (e.g., annual, defoliation as well as mortality), but multiple inconsistencies (e.g., polygons, not spatially comprehensive every year) with our data. The available ADS data (since 1997) for the conterminous US (Fig. 4) illustrate similar temporal patterns to our decline data (Fig. 2) across the regions demarcated in this study (Fig. 1). For both datasets, in the Lowland West there were low levels of disturbance before the turn of the century, followed by a peak between 2002 and 2004, and then a reduction in disturbance to levels through 2012 that are higher than the level before the turn of the century. In the Mountain West, disturbance levels began to rise earlier than for the Lowland West, peaking at approximately the same time in the early-2000s, and then not declining significantly. In the ADS data there is another peak in 2009 that appears absent from our data. Across the Northeast region we see three peaks post-2000 that are consistent in timing between the datasets. For the Southeast, levels are quite low in both datasets, but there is an ADS peak in 2001 that is not in our dataset.

Trends in mortality across the western US reported in the literature also support our decline results. Breshears et al. (2005) report

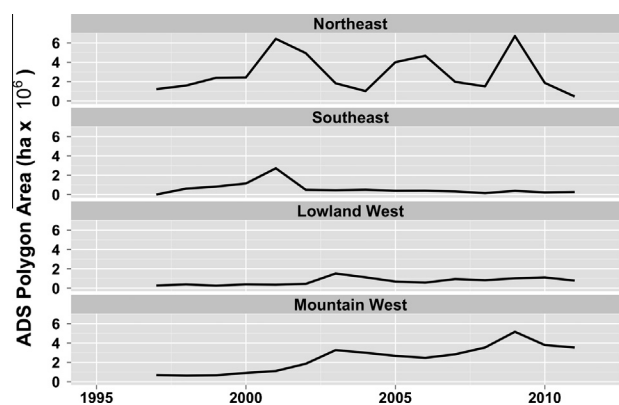


Fig. 4. Aerial Detection Survey (ADS) data summarized by the regional boundaries used in this study. Shown is ADS polygon area mapped by region.

widespread mortality (>90% of piñon pine at some sites) during an intense drought in the early 2000s, with peak die-off during 2002–2003, in an area approximately consistent with our Lowland West region. Williams et al. (2010) further describe an accelerated mortality period between 1997 and 2008 over a similar spatial extent, nearly identical to the period of our higher decline rates for the Lowland West. Importantly, our decline class includes not just mortality, but also partial canopy loss in response to severe drought, a phenomenon associated with juniper trees that are a prominent species group across the Lowland West region (Gaylord et al., 2013). This, in combination with the differences in spatial extent, prevent our rates of decline from being directly compared to rates associated with other, less spatially and more exclusive (i.e., mortality only) studies.

The Mountain West region hosts a diverse set of tree, insect, and disease species, all of which interact with a highly variable climate to result in more complex decline dynamics than in the Lowland West (Weed et al., 2013). Creeden et al. (2014) report lodgepole pine beetle-related mortality across nearly the full temporal range of our study, but with generally very low rates of mortality between the late 1980s and 2000 and peak rates occurring between 2001 and 2010, dependent on specific location. Other studies report variable specific timing of insect and disease activity depending on conifer tree and insect species and location, but are consistent with this study and with Creeden et al. (2014) regarding significant increases in activity starting in the mid-90s (Chapman et al., 2012; Meddens et al., 2012; Meddens and Hicke, 2014; Meigs et al., 2015). Moreover, decline not associated with insects has occurred in non-conifer-dominated forests, including a period of active aspen mortality between 1991 and 2007 (with a peak during 2000–2003; Hanna and Kulakowski, 2012).

Harvest rates (in cubic feet) across 10-year intervals from 1986–2011 reported by Oswalt et al. (2014, Table 41) exhibit no meaningful trend and vary by about 20% across the period, not unlike our harvest estimates. Moreover, akin to our results, throughout the study period, harvest rates are highest (maximum 12.2 billions of cubic feet) and somewhat variable (minimum 10.5 billion cubic feet) across the South (an area similar to our Southeast region). Also, harvest rates across the North (an area similar to our Northeast region) are reported to have been about 40% of those of the South, as in our study. Across the west harvest rates were generally lowest, with Rocky Mountain forests and Pacific Coast forests (most closely associated with our Lowland West region and our Mountain West regions, respectively) having less than 10% (Rocky Mountains) and 20–30% (Pacific Coast) of the rates associated with the Southeast region. From 1986 to 1996, rates of reported harvest in these areas declined by about 50%

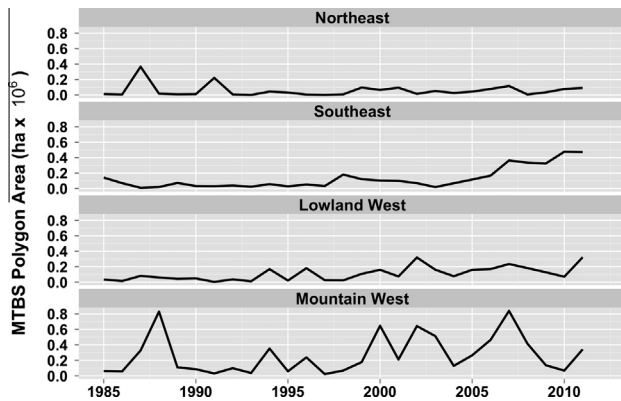


Fig. 5. MTBS fire data summarized by the regional boundaries used in this study. Shown is fire extent polygon area mapped by region.

and then remained at roughly the same levels through 2011, as in our study. Other studies have suggested that variability in harvest rates can be explained primarily through forest policy changes (Moeur et al., 2011) or economic drivers (Masek et al., 2013).

Summarizing the MTBS data for the western US, Dennison et al. (2014) report an increased number of large fires (above 400 ha) and area burned between 1984 and 2011. As with our results, the increases are greatest starting about 2000. Summarizing the same MTBS data to match our specific regional boundaries (Fig. 5), similar temporal patterns with our dataset are evident (Fig. 2). In the Lowland West and Mountain West regions greater area of fire activity occurred post-2000 than pre-2000, and the peak prior to 1990 in the latter region is consistent in both datasets. In the Northeast and Southeast regions, fire-affected areas are quite low throughout the period of observation. Differences between the two datasets were apparently related to the particular sample we selected; for example (data not shown), the MTBS dataset shows a post-2000 increase in fire activity in the Southeast that occurred in areas that by random chance were unsampled in our study.

Fire disturbances increased in western US at the turn of the century but remained a relatively small contributor to overall rates of forest disturbance in the west throughout the study period. However, because fires are so threatening to human lives and structures, are so costly to control, and remain an iconic symbol of the destructive forces of nature, they retain a dominant role in forest policy and management (Moeur et al., 2011), as they have since the dawn of the US Forest Service (Egan, 2009). In addition, these relatively low fire rates demonstrate the effectiveness of fire suppression and exclusion policies that have rendered a general fire deficit relative to historic conditions (Marlon et al., 2012). Despite the prominence of fire in the policy arena, the increasing rates of forest decline and climate-induced vulnerability to decline increasingly are the focus of both scientific investigation (Bréda and Peiffer, 2014; Mildrexler et al., submitted for publication) and public awareness (Rosner, 2015). In this context, our results support the need for increasing and urgent attention to that class of natural disturbances (Smith et al., 2014; McDowell et al., 2015).

4.2. Forest decline as a low intensity, multi-year phenomenon

Forest decline is a broadly defined term applied to largely climate-driven effects on forest health (Camarero et al., 2015). Decline is the result of complicated interacting factors that act at the local level, covering a range of effects from partial canopy defoliation to tree mortality (Lineras and Camarero, 2012; Vilà-Cabrera et al., 2013). Effects can be primary, such as hydraulic failure (Choat et al., 2012; Lineras and Camarero, 2012) and consequent

canopy defoliation that is either reversible (Bréda and Peiffer, 2014) or leads to mortality (Anderegg et al., 2015), or secondary, as in the case of reduced resin production that predisposes a tree to insect attack (Gaylord et al., 2013). Effects in a given tree may be abrupt or gradual (Amoroso et al., 2012) and not all trees in a local area are affected simultaneously such that within a given 30 m Landsat pixel (i.e., plot in our study) the effect may be cumulative, intensifying over many years (Meddens and Hicke, 2014; Meigs et al., 2015). Moreover, it is common that not all trees are affected within a given pixel, with, for example, 40–80% being the predominant range of mortality from the mountain pine beetle (Assal et al., 2014; Liang et al., 2014; Meddens and Hicke, 2014). When considering the impact of multiple stressors acting within a given pixel, decline can be slowly incremental (Meddens and Hicke, 2014), sometimes resulting in subtle year-to-year reflectance changes that accumulate over many years (e.g., Meigs et al., 2011; Table 4). This presents two special challenges: one with respect to monitoring and the other regarding how to summarize and report decline disturbance rates.

Landsat monitoring of forest decline represents a special case of monitoring relative to other disturbance agent classes because the magnitudes can be low relative to other agent classes, especially at an annual time-step (Fig. 3, top), and the effect can last for multiple consecutive years (Table 4). Using TimeSync we were able to reliably detect decline signals because we had ready access to a variety of tools for every plot. The toolset included simultaneous viewing of image chips that revealed the plot in the context of its pixel neighborhood, high resolution image snapshots available in Google Earth, ready access via toggling to multiple reflectance bands and indices for a truly multispectral interpretation, multiple ancillary datasets with approximate mapped locations of disturbance events for specific agent classes, and a human interpreter that could readily integrate the various information sources on a case-by-case basis. Designing an automated algorithm, which by definition relies on a higher degree of generalization, to replicate the human interpretation process will remain a significant challenge. Algorithms that explicitly track reflectance trends (e.g., Kennedy et al., 2010; Lambert et al., 2013; Brooks et al., 2014; Zhu and Woodcock, 2014), as opposed to those searching for higher magnitude anomalous reflectance departures from trends, undoubtedly hold the greatest promise for satisfying the new monitoring framework suggested by McDowell et al. (2015). In addition, algorithms that rely on denser temporal observations (rather than a single observation each year) may be able to suppress “noise” and extract subtler trends from the data.

With respect to reporting decline rates, most observed decline disturbances had multi-year durations, with the majority having durations of five or more years (Table 4). Because we summarized and reported annual decline disturbance rates for all years any given plot was affected, those plots were included in the rate calculation for all of the affected years (Fig. 2). If we exclude the duration component from our rate calculations, we isolate the “extensification” component of decline such that only newly affected areas (outside of the already affected 30 m plot) in a given year are included. However, doing so excludes the “intensification” component of the decline signal and thereby does not represent the actual area undergoing decline in any given year. We can address this challenge to reporting decline rates by summarizing and reporting both duration-weighted (including intensification) and duration-free (extensification only) rates that count only the first year of detection for decline disturbances. An important outcome is that by isolating the extensification component we also isolate the intensification component.

At the national scale, newly affected areas (extensification) generally accounted for less than 0.5% forest in any given year; the only exception being 2001 when the rate was nearly 0.7% (Fig. 6,

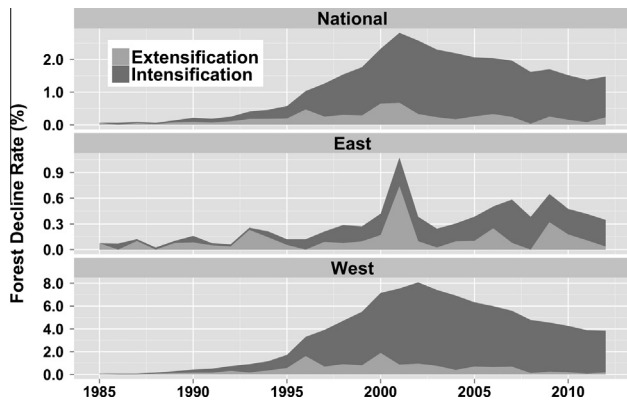


Fig. 6. Annual decline rate stratified by newly affected Landsat plots (extensification) and plots affected in a given year that were already affected the previous year (intensification). Shown are rates for the national level (top), the eastern regions combined (middle), and the western regions combined (bottom).

top). This is more similar to rates associated with the fire and other agent classes, and considerably less than rates associated with harvest. Not surprisingly, there are large differences between the eastern (combination of Northeast and Southeast), and western (combination of Lowland West and Mountain West) regions. In the east, intensification and extensification were approximately balanced over time (Fig. 6, middle). Across this region the intensification accounted for an average of only 59% (28.5% standard deviation among years) of the total decline rate. In the west however (Fig. 6 bottom), the large majority of detected decline was associated with intensification within areas already affected (Fig. 6, bottom). For this region intensification averaged 79% (21.7% standard deviation), which is highly consistent with the longer duration for decline occurrences, relative to the eastern regions.

The disturbance agent classes harvest and other also had some multi-year duration disturbance occurrences (Table 4). However, as these were a small proportion of the total number of occurrences, and the large majority of these had only one-year duration, we chose not to distinguish between intensification and extensification for these cases. The effect of this on our results is small, but should be recognized. The class other was dominated by land use conversions (Table 4). Although this could have been distinguished as a separate class for our analysis, we chose not to do so as this would have placed undue focus on conversion from forest to non-forest when, in fact, because of afforestation and reforestation after harvest forest land use has actually been increasing in the US (Oswalt et al., 2014).

5. Conclusions

This study presents the first direct comparison of annual trends among forest disturbance causal agent classes for the conterminous US as a whole and for five distinct forested regions of the country using consistent methods across classes and over a several-decade time period. Previously, national disturbance datasets derived using approximately consistent methods across distinct agent classes were either at too coarse a spatial or temporal resolution or temporal extent (Norman et al., 2013; Oswalt et al., 2014). Other national or greater level efforts focused on single agent classes (e.g., ADS insect and disease, MTBS fire) with methodological idiosyncrasies and inherent mapping biases (Eidenshink et al., 2007; Meddens et al., 2012), or only characterized disturbance in the aggregate so that specific temporal trends for individual causal agent disturbance classes could not be discovered (Hansen et al., 2013; Masek et al., 2013). The national forest

inventory program (Oswalt et al., 2014) has relied on a 5- to 10-year temporal revisit cycle and had no consistent measurement protocols across regions prior to 2000 (Schroeder et al., 2014).

Our results based on visual interpretation of Landsat time series, supported by high spatial resolution imagery in Google Earth and ancillary disturbance datasets from government agencies, indicate a shifting forest disturbance dynamic over the past several decades. Prior to the late-90s, disturbance patterns were driven largely by anthropogenic forces (e.g., harvest). Since the late-90s, natural forces (e.g., climate, insects and disease) have dominated national disturbance rates. Although a national phenomenon, increasing rates for forest decline have been concentrated in the western US where it is well documented that extended droughts have coupled with increasingly high temperatures to create increasingly stressed and vulnerable forests (Millar and Stephenson, 2015).

Landsat data have a 30 m spatial resolution, and it must be recognized that partial disturbances within a given pixel can occur for several consecutive years. Partial disturbances (e.g., forest thinning) can be challenging to detect, especially if they have one-year duration. Forest decline is commonly subtle in a given year, but because it tends to have a cumulative effect over several consecutive years it may be more detectable than short duration subtle disturbances. Forest decline, as a predominantly multi-year, cumulative phenomenon, should be analyzed and reported using its two components: intensification and extensification. This binary reporting avoids inflating the areal spread of decline while also enabling the full quantification of decline rates that include gradual and sometimes chronic forest changes associated with ongoing climatic stress. Despite the prominence of fire in the policy arena, the increasing rates of forest decline and climate-induced vulnerability to decline are increasingly the focus of both scientific investigation and public awareness. In this context, our results support the need for increasing and urgent attention to that class of natural disturbances.

Acknowledgements

We gratefully acknowledge the assistance of our TimeSync interpretation team including Alissa Moses, Peder Nelson, Eric Pfaff, Erik Haunreiter, Katie Blauvelt, Katie Brown, and Susmita Sen (who also helped with the TSA cluster stratification). This research was supported by NASA's Terrestrial Ecology Program and Carbon Cycle and Ecosystems Focus Area to Warren Cohen (NNH11AR291), and by the USFS Forest Inventory & Analysis Program and Region 6 Effectiveness Monitoring Program. We also acknowledge the helpful suggestions of the anonymous reviewers.

References

- Allen, C.D., Macalady, A.K., Chenchouni, H., et al., 2010. A global overview of drought and heat-induced tree mortality reveals emerging climate change risks for forests. *For. Ecol. Manage.* 259, 660–684.
- Amoroso, M.M., Daniels, L.D., Larson, B.C., 2012. Temporal patterns of radial growth in declining *Austrocedrus chilensis* forests in Northern Patagonia: the use of tree-rings as an indicator of forest decline. *For. Ecol. Manage.* 265, 62–70.
- Anderegg, W.R.L., Flint, A., Huang, C., et al., 2015. Tree mortality predicted from drought-induced vascular damage. *Nat. Geosci.* 8, 367–371.
- Assal, T.J., Sibold, J., Reich, R., 2014. Modeling a historical mountain pine beetle outbreak using Landsat MSS and multiple lines of evidence. *Remote Sens. Environ.* 155, 275–288.
- Banskota, A., Kayastha, N., Falkowski, M., et al., 2014. Forest monitoring using Landsat time-series data – a review. *Can. J. Remote Sens.* 40, 362–384.
- Braaten, J., Cohen, W.B., Yang, Z., 2015. Automated cloud and cloud shadow identification in Landsat MSS imagery for temperate ecosystems. *Remote Sens. Environ.* 169, 128–138.
- Bréda, N., Peiffer, M., 2014. Vulnerability to forest decline in a context of climate changes: new prospects about an old question in forest ecology. *Ann. For. Sci.* 71, 627–631.
- Breiman, L., 2001. Random forests. *Mach. Learn.* 45, 5–32.
- Breshhears, D.D., Cobb, N.S., Rich, P.M., et al., 2005. Regional vegetation die-off in response to global-change-type drought. *PNAS* 102, 15144–15148.

- Brooks, E.B., Wynne, R.H., Thomas, V.A., et al., 2014. On-the-fly massively multitemporal change detection using statistical quality control charts and Landsat data. *IEEE Trans. Geosci. Remote Sens.* 52, 3316–3332.
- Camarero, J.J., Gazol, A., Sangüesa-Barreda, G., et al., 2015. To die or not to die: early warnings of tree dieback in response to a severe drought. *J. Ecol.* 103, 44–57.
- Chapman, T.B., Veblen, T.T., Schoennagel, T., 2012. Spatiotemporal patterns of mountain pine beetle activity in the southern Rocky Mountains. *Ecology* 93, 2175–2185.
- Choat, B., Jansen, S., Brodribb, T.J., et al., 2012. Global convergence in the vulnerability of forests to drought. *Nature* 491, 752–756.
- Cohen, W.B., Goward, S.N., 2004. Landsat's role in ecological applications of remote sensing. *Bioscience* 54, 535–545.
- Cohen, W.B., Yang, Z., Kennedy, R.E., 2010. Detecting trends in forest disturbance and recovery using yearly Landsat time series: 2. TimeSync – tools for calibration and validation. *Remote Sens. Environ.* 114, 2911–2924.
- Cohen, W.B., Spies, T.A., Alig, R.J., Oetter, D.R., Maersperger, T.K., Fiorella, M., 2002. Characterizing 23 years (1972–1995) of stand replacement disturbance in western Oregon forests with Landsat imagery. *Ecosystems* 5, 122–137.
- Coulston, J.W., Moisen, G.G., Wilson, B.T., Finco, M.V., Cohen, W.B., Brewer, C.K., 2012. Modeling percent tree canopy cover across the United States: a Pilot study. *Photogramm. Eng. Remote Sens.* 78, 715–727.
- Creeden, E.P., Hicke, J.A., Buotte, P.C., 2014. Climate, weather, and recent mountain pine beetle outbreaks in the western United States. *For. Ecol. Manage.* 312, 239–251.
- Dennison, P.E., Brewer, S.C., Arnold, J.D., Moritz, M.A., 2014. Large wildfire trends in the western United States, 1984–2011. *Geophys. Res. Lett.* <http://dx.doi.org/10.1002/2014GL059576> (AGU Publications).
- Edwards, D.P., Tobias, J.A., Sheil, D., Meijaard, E., Laurance, W.F., 2014. Maintaining ecosystem function and services in logged tropical forests. *Trends Ecol. Evol.* 29, 511–520.
- Egan, T., 2009. *The Big Burn: Teddy Roosevelt and the Fire that Saved America*, first ed. Houghton, Mifflin, Harcourt Publishing Company, NY, 336 p.
- Eidenshink, J., Schwind, B., Brewer, K., Zhu, Z., Quayle, B., Howard, S., 2007. A project for monitoring trends in burn severity. *Fire Ecol. Spec. Issue* 3, 3–21.
- Gaylord, M.L., Kolb, T.E., Pockman, W.T., Plaut, J.A., Yezzer, E.A., Macalady, A.K., Pangle, R.E., McDowell, N.G., 2013. Drought predisposes piñon-juniper woodlands to insect attacks and mortality. *New Phytol.* 198, 567–578.
- Gómez, C., White, J.C., Wulder, M.A., 2011. Characterizing the state and processes of change in a dynamic forest environment using hierarchical spatio-temporal segmentation. *Remote Sens. Environ.* 115, 1665–1679.
- Hanna, P., Kulakowski, D., 2012. The influences of aspen dieback. *For. Ecol. Manage.* 274, 91–98.
- Hansen, M.C., Potapov, P.V., Moore, R., et al., 2013. High-resolution global maps of 21st-century forest cover change. *Science* 342, 850–853, with supplementary materials (www.sciencemag.org/content/342/6160/850/suppl/DC1).
- Healey, S.P., Zhiqiang, Y., Cohen, W.B., Pierce, J., 2006. Application of two regression-based methods to estimate the effects of partial harvest on forest structure using Landsat data. *Remote Sens. Environ.* 101, 115–126.
- Huang, C., Goward, S.N., Masek, J.G., Thomas, N., 2010. An automated approach for reconstructing recent forest disturbance history using dense Landsat time series stacks. *Remote Sens. Environ.* 114, 183–198.
- Kennedy, R.E., Yang, Z., Cohen, W.B., 2010. Detecting trends in forest disturbance and recovery using yearly Landsat time series: 1. LandTrendr – temporal segmentation algorithms. *Remote Sens. Environ.* 114, 2897–2910.
- Kennedy, R.E., Yang, Z., Cohen, W.B., Pfaff, E., Braaten, J., Nelson, P., 2012. Spatial and temporal patterns of forest disturbance and regrowth within the area of the Northwest Forest Plan. *Remote Sens. Environ.* 122, 117–133.
- Kennedy, R.E., Yang, Z., Braaten, J., Copass, C., Anotova, N., Jordan, C., Nelson, P., 2015. Attribution of disturbance change agent from Landsat time-series in support of habitat monitoring in the Puget Sound region, USA. *Remote Sens. Environ.*
- Lambert, J., Drenou, C., Denux, J.-P., et al., 2013. Monitoring forest decline through remote sensing time series analysis. *GISci. Remote Sens.* 50, 437–457.
- Liang, L., Hawbaker, T.J., Chen, Y., et al., 2014. Characterizing recent and projecting future potential patterns of mountain pine beetle outbreaks in the Southern Rocky Mountains. *Appl. Geogr.* 55, 165–175.
- Lineras, J.C., Camarero, J.J., 2012. From pattern to process: linking intrinsic water-use efficiency to drought-induced forest decline. *Glob. Change Biol.* 18, 1000–1015.
- Marlon, J.R., Bartlein, P.J., Gavin, D.G., et al., 2012. Long-term perspective on wildfires in the western USA. *PNAS* 109, E535–E543.
- Masek, J.G., Goward, S.N., Kennedy, R.E., et al., 2013. United States forest disturbance trends observed using Landsat time series. *Ecosystems*. <http://dx.doi.org/10.1007/s10021-013-9669-9>.
- Masek, J.G., Huang, C., Cohen, W.B., et al., 2008. North American forest disturbance mapped from a decadal Landsat record: methodology and initial results. *Remote Sens. Environ.* 112, 2914–2926.
- McDowell, N., Coops, N.C., Beck, P.S.A., et al., 2015. Global satellite monitoring of climate-induced vegetation disturbances. *Trends Plant Sci.* 20, 114–123.
- Meddens, A.J.H., Hicke, J.A., 2014. Spatial and temporal patterns of Landsat-based detection of tree mortality caused by a mountain pine beetle outbreak in Colorado, USA. *For. Ecol. Manage.* 322, 78–88.
- Meddens, A.J.H., Hicke, J.A., Ferguson, C.A., 2012. Spatiotemporal patterns of observed bark beetle-caused tree mortality in British Columbia and the western United States. *Ecol. Appl.* 22, 1876–1891.
- Meigs, G., Kennedy, R.E., Cohen, W.B., 2011. A Landsat time series approach to characterize bark beetle and defoliator impacts on tree mortality and surface fuels in conifer forests. *Remote Sens. Environ.* 115, 3707–3718.
- Meigs, G.W., Kennedy, R.E., Gray, A.N., Gregory, M.J., 2015. Spatiotemporal dynamics of recent mountain pine beetle and western spruce budworm outbreaks across the Pacific Northwest Region, USA. *For. Ecol. Manage.* 339, 71–86.
- Mildrexler, D., Yang, Z., Cohen, W.B., submitted for publication. A forest vulnerability index based on drought and high temperatures. *Remote Sens. Environ.*
- Millar, C.I., Stephenson, N.I., 2015. Temperate forest health in an era of emerging megadisturbance. *Science* 349, 823–826.
- Moer, M., Ohmann, J.L., Kennedy, R.E., Cohen, W.B., Gregory, M.J., Yang, Z., Roberts, H.M., Spies, T.A., Fiorella, M., 2011. Northwest Forest Plan – The first 15 years (1994–2008): Status and Trends of Late-successional and Old-growth Forests. *Gen. Tech. Rep. PNW-GTR-853*. U.S. Department of Agriculture, Forest Service, Pacific Northwest Research Station, Portland, OR, 48 p.
- Norman, S.P., Hargrove, W.W., Spruce, J.P., et al., 2013. Highlights of Satellite-based Forest Change Recognition and Tracking using the ForWarn System. *Gen. Tech. Rep. SRS-180*. U.S. Department of Agriculture Forest, Asheville, NC, 30 p.
- Olofsson, P., Foody, G.M., Stehman, S.V., et al., 2013. Making better use of accuracy data in land change studies: estimating accuracy and area and quantifying uncertainty using stratified estimation. *Remote Sens. Environ.* 129, 122–131.
- Omerik, J.M., 1987. Ecoregions of the conterminous United States. *Ann. Assoc. Am. Geogr.* 77, 118–125.
- Oswalt, S.N., Smith, W.B., Miles, P.D., et al., 2014. Forest Resources of the United States, 2012: A Technical Document Supporting the Forest Service 2015 Update of the RPA Assessment. *Gen. Tech. Rep. WO-91*. U.S. Department of Agriculture, Forest Service, Washington Office, Washington, DC, 218 p.
- Pflugmacher, D., Cohen, W.B., Kennedy, R.E., 2012. Comparison between Landsat-derived disturbance history and lidar to predict current forest structure. *Remote Sens. Environ.* 122, 146–165.
- Powell, S.L., Cohen, W.B., Healey, S.P., et al., 2010. Quantification of live aboveground forest biomass dynamics with Landsat time-series and field inventory data: a comparison of empirical modeling approaches. *Remote Sens. Environ.* 114, 1053–1068.
- Powell, S.L., Cohen, W.B., Kennedy, R.E., et al., 2014. Empirical observation of trends in biomass loss due to disturbance in the conterminous U.S.: 1986–2004. *Ecosystems* 17, 142–157.
- Rosner, H., 2015. The bug that's eating the woods. *Natl. Geogr. Mag.* April 2015.
- Roy, D.P., Wulder, M.A., Loveland, T.R., et al., 2014. Landsat-8: science and product vision for terrestrial global change research. *Remote Sens. Environ.* 145, 154–172.
- Ruefenacht, B., Finco, M.V., Nelson, M.D., Czaplewski, R., Helmer, E.H., Blackard, J.A., et al., 2008. Conterminous U.S. and Alaska forest type mapping using forest inventory and analysis data. *Photogramm. Eng. Remote Sens.* 74, 1379–1388.
- Running, S.W., 2008. Ecosystem disturbance, carbon, and climate. *Science* 321, 652–653.
- Särndal, C.E., Swensson, B., Wretman, J., 1992. *Model-Assisted Survey Sampling*. Springer-Verlag, New York.
- Schroeder, T.A., Healey, S.P., Moisen, G.G., et al., 2014. Improving estimates of forest disturbance by combining observations from Landsat time series with US Forest Service Forest Inventory and Analysis data. *Remote Sens. Environ.* 154, 61–73.
- Seidl, R., Schelhaas, M.-J., Rammer, W., Verkerk, P.J., 2014. Increasing forest disturbance in Europe and their impacts on carbon storage. *Nature Clim. Change* 4, 806–810.
- Skakun, R.S., Wulder, M.A., Franklin, S.E., 2003. Sensitivity of the thematic mapper enhanced wetness difference index to detect mountain pine beetle red-attack damage. *Remote Sens. Environ.* 86, 433–443.
- Smith, A.M.S., Kolden, C.A., Tinkham, W.T., et al., 2014. Remote sensing the vulnerability of vegetation in natural terrestrial ecosystems. *Remote Sens. Environ.* 154, 322–337.
- Utter, J., Maltamo, M., Kuusela, K., 1996. Impact of forest management history on the state of forests in relation to natural forest succession: comparative study, North Karelia, Finland vs. Republic of Karelia, Russian Federation. *For. Ecol. Manage.* 83, 71–85.
- Vilà-Cabrera, A., Martínez-Vilalta, J., Galiano, L., et al., 2013. Patterns of forest decline and regeneration across Scots pine populations. *Ecosystems* 16, 323–335.
- Vogelmann, J.E., Kost, J.R., Tolk, B., et al., 2011. Monitoring landscape change for LANDFIRE using multi-temporal satellite imagery and ancillary data. *IEEE J. Sel. Top. Appl. Earth Observ. Remote Sens.* 4, 252–264.
- Weed, A.S., Ayres, M.P., Hicke, J.A., 2013. Consequences of climate change for biotic disturbances in North American forests. *Ecol. Monogr.* 83, 441–470.
- Westerling, A.L., Hidalgo, H.G., Cayan, D.R., Swetnam, T.W., 2006. Warming and earlier spring increases western U.S. forest wildfire activity. *Sci. Express*. <http://dx.doi.org/10.1126/science.1128834>.
- Williams, A.P., Allen, C.D., Millar, C.I., et al., 2010. Forest responses to increasing aridity and warmth in the southwestern United States. *Proc. Natl. Acad. Sci.* 107, 21289–21294.
- Woodcock, C.E., Allen, R., Anderson, M., et al., 2008. Free access to Landsat data. *Science* 320, 1011.
- Zhu, Z., Woodcock, C.E., 2014. Continuous change detection and classification of land cover using all available Landsat data. *Remote Sens. Environ.* 144, 152–171.